

New Metal Complexes Derived from Heterocyclic Schiff-base Ligand; Preparation, Structural Investigation and Biological Activity

Hind I. Khaleel, Baidaa K. Al-Rubaye*

Department of Chemistry, College of Education for Pure Science (Ibn Al-Haitham), University of Baghdad, Baghdad, Iraq

Received: 12th July, 2022; Revised: 20th July, 2022; Accepted: 24th August, 2022; Available Online: 25th September, 2022

ABSTRACT

The formation of a Schiff-base with N₂O₂ donor atoms derived from the hydrazine segment and its metal complexes are reported. The Schiff-base ligand; N'-((1R,2S,4R,5S,Z)-2,4-diphenyl-3-azabicyclo[3.3.1]nonan-9-ylidene)furan-2-carbohydrazide (HL) was prepared from the reaction of furan-2-carbohydrazide with (1R, 2R, 4R, 5S)-2,4-diphenyl-3-azabicyclo[3.3.1]nonan-9-one (M1) in ethanol medium. The reaction of the title ligand with selected metal ions Cr(III), Mn(II), Ni(II), Cu(II), Zn(II) and Cd(II) gave complexes with the general formula [M(L)Cl₂], (where: M = Cr(III), Mn(II), Ni(II), Cu(II), Zn(II) and Cd(II)). Spectroscopic analyses Fourier transform infrared (FT-IR), Nuclear Magnetic Resonance (NMR) Carbon-13 nuclear magnetic resonance (¹H- and ¹³C-NMR), mass and electronic spectroscopy and atomic absorption) along with elemental microanalysis (C.H.N), chloride percentage, conductivity measurements, magnetic moments and melting point were used to establish the identity of ligand and complexes. The biological activity of the synthesized compounds towards bacterial strains (G⁺ and G⁻) was investigated.

Keywords: Biological evaluation, Heterocyclic ligand, Metal complexes, Schiff base, Structural analyses.

International Journal of Drug Delivery Technology (2022); DOI: 10.25258/ijddt.12.3.68

How to cite this article: Khaleel HI, Al-Rubaye BK. New Metal Complexes Derived From Heterocyclic Schiff-Base Ligand; Preparation, Structural Investigation And Biological Activity. International Journal of Drug Delivery Technology. 2022;12(3):1341-1346.

Source of support: Nil.

Conflict of interest: None

INTRODUCTION

The Mannich reaction is a model of the multicomponent reaction pathway (MCRs). This type of reaction is used to produce a range of natural product components, including the formation of heterocyclic phenanthridines derivatives,^{1,2} and to be used in medicine.³ The Mannich reaction involves the mixing of three components: an aldehyde, a ketone (one acidic hydrogen atom), and an amine (a primary or secondary).⁴⁻⁶ Following the first orientation and the removal of the water molecule, the interaction of the amine with the primary carbonyl produced an iminium ion. The iminium ion then forms the Mannich base in an aldol-like reaction with the degradable molecule *via* the alpha carbon.⁷ Researchers that employed synthetic methodologies in the formation of Mannich bases have accomplished the goal of reducing reaction steps and achieving a cleaner as well as ecologically friendly reaction by adhering to the green chemistry approach. These methods include uses; (i) an aqueous medium, (ii) ionic liquids, (iii) avoiding solvents and/or catalysts, (iv) the use of ultrasonography and ultrasound methods, (v) catalysts that are biodegradable and/or reusable.⁸ Mannich compounds can be used as scavengers for the removal of heavy elements from

water-stream and wastewater treatment⁹ There are a pile of publications that include the formation of organic ligands derived from Mannich bases and their complexes with a range of elements.^{10,11} Furthermore, the Mannich-compounds have several applications, including their role in environmental, agricultural, analytical chemistry, polymer chemistry, antibacterial, and anticancer agents. Accordingly, this paper describes the formation and structural characterization of one multidentate heterocyclic ligand N'-((1R,2S, 4R,5S,Z)-2,4-diphenyl-3-azabicyclo[3.3.1]nonan-9-ylidene)furan-2-carbohydrazide (HL) and its metal complexes. The antibacterial of prepared compounds were also explored.

Experimental

Materials and Procedures

The used materials and reagents in this study were purchased commercially and used as received additional purification.

Physical Measurements

The measurement of melting points were conducted using a Stuart SMP10 thermoelectric instrument. Fourier transform infrared (FT-IR) spectral data were obtained as KBr and CsI discs using a Biotic 600 FT-IR and a Shimadzu 8400s FT-IR

*Author for Correspondence: baidaaakareem83@gmail.com

spectrophotometer. The Bruker-500 MHz was used to collect Proton and Carbon-13 nuclear magnetic resonance (^1H and ^{13}C NMR) spectra of ligand at 298 K using DMSO- d_6 solutions (Figures 1 and 2). TMS was used as an internal reference for ^1H -NMR and chemical shifts were reported in ppm from trimethylsilyl group (TMS). Electrospray (ES) mass spectra were acquired with an Linear Ion Trap-Fourier Transform Ion Cyclotron Resonance Mass Spectrometer (LTQ-FT) mass spectrometer (Thermo Fisher Scientific) (Figure 3). Electronic spectral data of ligand and complexes were measured at room temperature between 200–1100 nm for 10–3 M solutions using a Shimadzu 1800 UV-vis spectrophotometer. Chloride percentage for complexes was evaluated by a 686-titro-665 Dosimat-Metrohm Swiss process. Eutech Instruments Co, 150 digital conductivity meters was used to find out the conductance of complexes in Dimethyl sulfoxide (DMSO) solutions. Magnetic susceptibility for paramagnetic complexes was concluded at 298 K using a Sherwood scientific sensitivity balance. Elemental analysis (C.H.N.) for compounds were conducted on an Eager 300 for EA1112. The evaluation of ligand and its metal complexes towards *Escherichia coli*, *Pseudomonas aeruginosa*, *Staphylococcus aureus* and *Staphylococcus bacillus* was investigated at the College of Science, University of Baghdad, Iraq.

Synthesis

Preparation of M_1 and A

A published method included in^{6, 10-12} was used to isolate M_1 .

Formation of (1R,2R,4R,5S)-2,4-diphenyl-3-azabicyclo[3.3.1]nonan-9-one (M_1)

A three-component mixture of benzaldehyde (2.65 mL, 0.025 mmol), ammonium acetate (1g, 12.98 mmol) and cyclohexanone (1.34 mL, 12.96 mmol) [2:1:1] in ethanol (20 mL) was mixed and heated for 6 hours between 30–40°C. After cooling at room temperature, the white crystals that formed were filtered off, and washed with 5/mL of ethanol and 10/mL of diethyl ether. Yield: 1.25g (93%), m.p = 108–110 °C. FT-IR data (cm^{-1}), 3317 ν (N–H), 3032 ν (C–H) aromatic., 2920 and 2850 ν (C–H) aliphatic, 1716 ν (C=O), 1585 and 1558 ν (C=C), 1489 δ (N–H).

Preparation of furan-2-carbohydrazide(A)

To a mixture of 2-furoyl chloride (0.75/mL, 7.61mmol) in benzene (10/mL) in an ice bath was added slowly hydrazinemonohydrate (0.23mL, 7.41mmol). The reaction mixture was stirred for 90 min and heated at reflux for 30 min. A white precipitate was crushed out which was filtered off, washed with benzene (5/mL) and diethyl ether (10/mL). Yield: 0.51g (53%), m.p = 240–243 °C. FT-IR data (cm^{-1}), 3306 ν (N–H), 3119 ν (C–H) arom., 2970 ν (C–H) aliph., 1635 ν (C=O), 1591 ν (C=C), 1519 δ (N–H).

Synthesis of Ligand (HL)

Preparation of N' -((1R,2S,4R,5S,Z)-2,4-diphenyl-3-azabicyclo[3.3.1]nonan-9-ylidene) furan-2-carbohydrazide (HL)

To a solution of M_1 (0.231 g, 0.79 mmol) in ethanol (10 mL) with two drops of conc. HCl was added slowly with stirring A (0.1g, 0.79mmol) in ethanol (10mL). The mixture was heated at 30–40 °C for 6 h. A white solid that collected by filtration washed with diethyl ether (5mL). Yield: 0.19g (60%), m.p = 210–212 °C. Table 1 tabulates the required data for precursors and ligands. FT-IR data (cm^{-1}), 3443, 3155 ν (N–H) amide, 3024 ν (C–H) arom., 2970 ν (C–H) alip., 1674 ν (C=O) amide, 1639 ν (C=N), 1593 ν (C=C) arom., 1469 δ (N–H), 1388 ν (C–N), 1226 ν (C–O). ^1H NMR (400 MHz, DMSO- d_6) is shown in Figure 1 and reported the following; 1.25 (4H, m, $\text{C}_{9,9}$ -H); 1.63 (2H, t, $J_{\text{HH}} = 4\text{Hz}$, C_{10} -H); 2.35 (3H, t, $J_{\text{HH}} = 6\text{Hz}$, $\text{C}_{8,8}$ -H); 2.86(1H, s, N-H); 3.27 (2H, d, $J_{\text{HH}} = 4\text{Hz}$, $\text{C}_{7,7}$ -H); 6.51 (1H, m, C_{14} -H); 7.31 (7H, m, $\text{C}_{1,1}, \text{C}_{2,2}, \text{C}_{6,6}, \text{C}_{13}$ -H); 7.61 (4H, dd, $\text{C}_{3,3}, \text{C}_{5,5}$ -H); 7.44 (1H, d, $J_{\text{HH}} = 7.2\text{Hz}$, C_{15} -H); 10.38 (N- $H_{\text{hydrazinic}}$). ^{13}C NMR (100 MHz, DMSO- d_6), Figure 2, showed the following; 21.04 (C_{10}); 29.01 ($\text{C}_{9,9}$); 53.72 ($\text{C}_{8,8}$); 64.23 ($\text{C}_{7,7}$); 112.27 (C_{13}); 117.53 (C_{14}); 123.27 ($\text{C}_{1,1}$); 127.37 ($\text{C}_{2,2}, \text{C}_{6,6}$); 127.53 ($\text{C}_{3,3}, \text{C}_{5,5}$); 128.73 ($\text{C}_{4,4}$); 133.23 (C_{12}); 140.21(C_{15}); 161.22 (C=N); 164.53 (C=O). The ES MS (+) of HL, Figure 3, revealed the mass ion of the molecular peak at $m/z = 400.4$ ($M+1$)⁺ for $\text{C}_{25}\text{H}_{26}\text{N}_3\text{O}_2$, requires = 399.49. Peaks detected at $m/z = 291.4, 262.4, 194.8, 144.1, 106.1, 78.2$ and 56.1 were assigned to $[\text{M}-(\text{C}_4\text{H}_{14}\text{NO}_2)]$, $[\text{M}-(\text{C}_4\text{H}_{14}\text{NO}_2)+(\text{N}_2\text{H})]$, $[\text{M}-(\text{C}_4\text{H}_{14}\text{NO}_2)+(\text{N}_2\text{H})+(\text{C}_5\text{H}_{14})]$, $[\text{M}-(\text{C}_4\text{H}_{14}\text{NO}_2)+(\text{N}_2\text{H})+(\text{C}_5\text{H}_{14})+(\text{C}_4\text{H}_2)]$, $[\text{M}-(\text{C}_4\text{H}_{14}\text{NO}_2)+(\text{N}_2\text{H})+(\text{C}_5\text{H}_{14})+(\text{C}_4\text{H}_2)+(\text{C}_8\text{H}_{10})]$, $[\text{M}(\text{C}_4\text{H}_{14}\text{NO}_2)+(\text{N}_2\text{H})+(\text{C}_5\text{H}_{14})+(\text{C}_4\text{H}_2)+(\text{C}_8\text{H}_{10})+(\text{C}_2\text{H}_4)]$ and $[\text{M}-(\text{C}_4\text{H}_{14}\text{NO}_2)+(\text{N}_2\text{H})+(\text{C}_5\text{H}_{14})+(\text{C}_4\text{H}_2)+(\text{C}_8\text{H}_{10})+(\text{C}_2\text{H}_4)+(\text{C}_4\text{H}_2)]$, respectively.

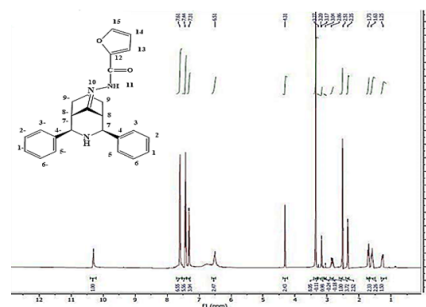


Figure 1: ^1H -NMR of HL ligand in DMSO- d_6 .

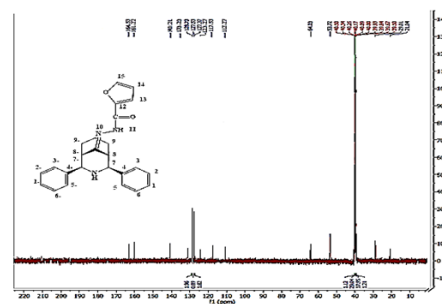


Figure 2: ^{13}C -NMR of HL ligand in DMSO- d_6 .

Table 1: Microanalyses results and other data for precursors and the ligand

Comp.	Empirical formula	M.wt g/ mol	Yield (%)	m.p. °C	Colour	Found/(Calc.)%			
						C	H	N	O
M1	C ₂₀ H ₂₁ NO	291.39	93	108–110	White	(82.44) 82.89	(7.26) 7.88	(4.48) 4.85	(5.49) 5.90
A	C ₅ H ₆ N ₂ O ₂	126.12	53	240–243	White	(47.62) 47.23	(4.80) 5.03	(22.21) 22.53	(25.37) 25.61
HL	C ₂₅ H ₂₅ N ₃ O ₂	399.49	60	210–212	White	(75.16) 74.06	(6.31) 6.69	(10.52) 10.70	(8.01) 7.83

Table 2: Microanalyses and physical properties of HL complexes

Complex	M.wt	Yield	Colour	m.p	Micro-analysis; Found and (calculated)%					
					C	H	N	O	M	Cl
[Cr(HL) ₂ Cl ₂]Cl	957.33	49	Green	292*	(62.73) 62.58	(5.26) 5.68	(8.78) 8.34	(6.68) 6.49	(5.43) 5.27	(11.11) 11.36
[Mn(HL) ₂ Cl ₂]	924.83	53	Brown	320*	(64.94) 64.77	(5.45) 5.23	(9.09) 9.89	(6.92) 7.84	(5.94) 4.69	(7.67) 7.45
[Ni(HL) ₂ Cl ₂]	928.58	46	Deep yellow	287*	(64.67) 64.88	(5.43) 5.29	(9.05) 9.89	(6.89) 7.01	(6.32) 6.53	(7.64) 7.78
[Cu(HL) ₂]Cl ₂	933.43	55	Brown	263*	(64.34) 64.12	(5.40) 5.19	(9.00) 9.25	(6.68) 7.82	(6.81) 7.02	(7.60) 7.32
[Zn(HL) ₂]Cl ₂	935.27	54	White	308*	(64.21) 64.09	(5.39) 5.45	(8.99) 9.07	(6.84) 6.89	(6.99) 7.08	(7.58) 7.50
[Cd(HL) ₂]Cl ₂	982.30	52	White	335*	(61.14) 60.87	(5.13) 5.43	(8.56) 8.97	(6.51) 6.32	(11.44) 11.87	(7.22) 7.04

* = Decomposition temperature.

Table 3: FT-IR data (cm⁻¹) of HL and its complexes.

Compound	$\nu(N-H)$	$\nu(C=O)$	$\nu(C=N)$	$\nu(C=C)$	$\delta(N-H)$	$\nu(C-N)$	$\nu(M-O)$	$\nu(M-N)$	$\nu(M-Cl)$
		amid	imine	arom					
HL	3443 3155	1674	1639	1593	1469	1388	-	-	-
[Cr(HL) ₂ Cl ₂]Cl	3479 3414 3317 3236	1639	1616	1492	1450	1346	522	477	266
[Mn(HL) ₂ Cl ₂]	3442 3417 3236 3113	1639	1600	1570	1469	1361	513	470	260
[Ni(HL) ₂ Cl ₂]	3470 3313 3240 3124	1631	1600	1516	1473	1357	594	455	264
[Cu(HL) ₂]Cl ₂	3474 3414 3236 3132	1635	1616	1519	1477	1361	594	470	-
[Zn(HL) ₂]Cl ₂	3441 3230 3158	1658	1604	1508	1462	1388	513	455	-
[Cd(HL) ₂]Cl ₂	3443 3389 3275	1657	1631	1589	1458	1388	513	422	-

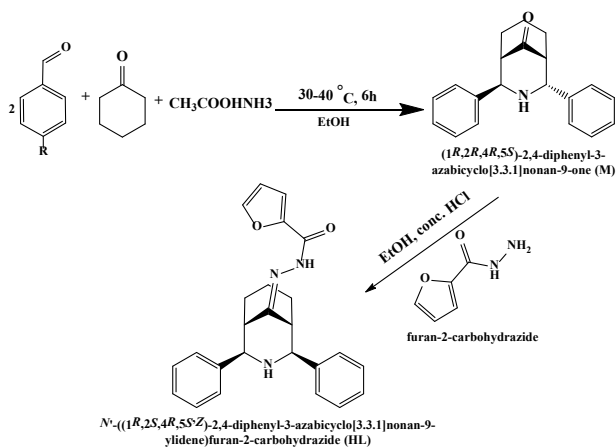
Table 4: Electronic data of HL complexes in DMSO solutions

Comp.	Band Position λ_{nm}	Wave number (cm^{-1})	Extinction coefficient ϵ_{max}^{3-1-1} ($dm^3 mol^{-1} cm^{-1}$)	Assignment	$A_m S.cm^2$ $mole^{-1}$	Suggested geometry
HL	271	36900	1858	$\pi \rightarrow \pi^*$		
[Cr(HL) ₂ Cl ₂]Cl	265	1084	37735	L.F*	37.06	Distorted Octahedral
	349	170	28865	C.T*		
	758	27	13192	$^4A_{2g} \rightarrow ^4T_{2g}^{(F)}$		
	858	27	11655	$^4A_{2g} \rightarrow ^4T_{1g}, ^4E_g$		
[Mn(HL) ₂ Cl ₂]	266	1337	37593	L.F	7.24	Distorted Octahedral
	725	8	13793	$^2E_g^{(G)} \rightarrow ^4T_{1g}^{(F)}$		
[Ni(HL) ₂ Cl ₂]	268	13	37313	L.F	13.89	Distorted Octahedral
	330	1013	30303	L.F		
	346	1450	28901	C.T		
	810	5	12345	$^3A_{2g} \rightarrow ^3T_{1g}^{(F)}$		
[Cu(HL) ₂]Cl ₂	266	1061	37593	L.F	30.21	Distorted square planar
	857	37	11668	$^2B_{1g} \rightarrow ^2A_{2g}$		
[Zn(HL) ₂]Cl ₂	263	581	28022	L.F	37.45	Distorted Tetrahedral
[Cd(HL) ₂]Cl ₂	265	978	37735	L.F	35.29	Distorted Tetrahedral
	348	732	28735	C.T		

*L.F=ligand field, C.T=charge transfer.

Table 5: The bacterial activity of HL and its complexes.

Compound	<i>Staphylococcus aureus</i>	<i>Bacillus subtilis</i>	<i>Escherichia coli</i>	<i>Pseudomonas aeruginosa</i>
HL	24	25	28	25
[Cr(HL) ₂ Cl ₂]Cl	32	32	23	26
[Mn(HL) ₂ Cl ₂]	27	26	20	26
[Ni(HL) ₂ Cl ₂]	21	20	23	29
[Cu(HL)]Cl ₂	27	32	22	32
[Zn(HL) ₂]Cl ₂	21	25	28	25
[Cd(HL) ₂]Cl ₂	29	29	24	25

**Scheme 1:** A synthetic pathway for HL.

Synthesis of HL complexes

To a solution of HL (0.1 g, 0.25 mmol) in (10 mL) of ethanol was added to a mixture of metal chloride (0.03 g, 0.112 mmol) dissolved in a minimum amount of ethanol. The mixture was refluxed for 4 hours and a colored solid that crushed out was

collected by filtered, then washed with 5 mL of ethanol and 10 mL of diethyl ether. Table 2 shows elemental microanalyses of precursors and ligand, as well as colors, yields, and melting points.

RESULTS AND DISCUSSION

The ligand was prepared following a condensation reaction between (1R, 2R, 4R, 5S)-2,4-diphenyl-3-azabicyclo[3.3.1]nonan-9-one with furan-2-carbohydrazide (Scheme 1). The reaction was carried out in ethanol at reflux. The free ligand is soluble with stirring in drug master files (DMF) and DMSO and boiling ethanol and methanol. It is sparingly soluble in other organic solvents. The prepared compounds were characterized by the C.H.N. (Tables 1 and 2), FT-IR (Table 3) and UV-Vis (Table 4) spectroscopy, ¹H- and ¹³C-NMR spectra and mass spectroscopy.

The monomeric complexes of the ligand with Cr(III), Cu(II), Ni(II), Mn(II), Zn(II), and Cd(II) metal chlorides were prepared from mixing a 2 mole of the ligand with 1 mole of the metal ion using ethanol solvent at reflux (Scheme 2). The results showed complexes that have six-coordinated donor atoms with

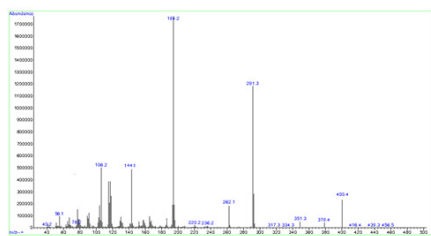
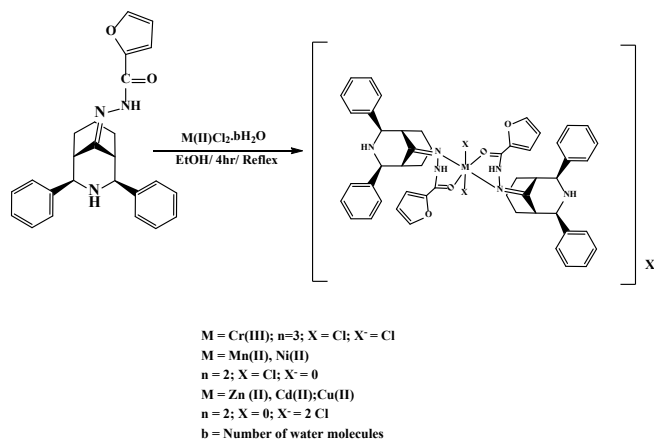


Figure 3: ES(+) mass spectrum of HL.



Scheme 2: A synthetic pathway for HL complexes.

the general formula $[M(HL)_2Cl_2]$ with Cr(III), Mn(II), Ni(II) and the four-coordinate complexes with the general formula $[M(HL)_2]$ with Cu(II), Zn(II) and Cd(II) ions. The suggested formulae are well supported by physicochemical evidence. The vibrational FTIR data and their assignments for compounds are presented in Table 3. The UV-vis data for compounds are included in Table 4.

FT-IR data

Table 3 lists the FTIR spectral data of precursors, ligand and its monomeric complexes, as well as their interpretation. The HL spectrum contains bands related to $\nu(N-H)$ amide,¹³ $\nu(C=O)$ amide^{14,15} and $(C=N)$ imine¹⁶ at 3443, 3155, 1674 and 1639 cm^{-1} , respectively. The FTIR data of complexes indicated bands in around 1639–1657 cm^{-1} and about 1631–1600 cm^{-1} , which were attributed to $\nu(C=O)$ amide and $\nu(C=N)$ stretching, respectively. The detected bands showed a reduced bond order, compared to the unbound ligand, confirming the involvement of the imine moieties in the coordination to the metal core.¹⁷ Bands recorded in the range 513–594 in the spectra of complexes were related to the $\nu(M-O)$. Bands observed around 260–266 in the spectra of $[Cr(HL)_2Cl_2]Cl$, $[Mn(HL)_2Cl_2]$, $[Ni(HL)_2Cl_2]$, $[Cu(HL)_2]Cl_2$, $[Zn(HL)_2]Cl_2$ and $[Cd(HL)_2]Cl_2$ are attributed to $\nu(M-Cl)$.¹⁸

UV-visible spectra and conductance

The UV-vis data for HL displays a peak at 271 nm related to an overlap of $\pi \rightarrow \pi^*$ and $\pi \rightarrow n$ transitions.^{19,20,21} The spectra of HL complexes showed a peak correlated to the ligand field. The spectrum of Cr(III)-complex exhibited bands at 758 and 858 nm related to ${}^4A_2g(F) \rightarrow {}^4T_2g(F)$, ${}^4A_2g \rightarrow {}^2T_1g$, 4Eg , respectively indicating the geometry about the Cr atom is a

distorted octahedral.²² The Mn(II) complex showed a peak at 725 nm related to ${}^2Eg(G) \rightarrow {}^4T_1g(F)$, respectively.²³ This peak indicated the possible geometry about the Mn atom is a distorted octahedral geometry.²⁴ The ${}^3A_2g \rightarrow {}^3T_1g(F)$ transitions of the Ni(II) complex is detected at 810 nm, which supported the octahedral structure around the metal centre.²⁵ The Cu(II) complex exhibited a band that assigned to ${}^2B_1g \rightarrow {}^2A_2g$ transition, corresponding to distorted square planar Cu(II) complex.²⁶ The spectral data of the Zn(II) and Cd(II) complexes showed bands at 263 and 265 nm, respectively. These bands are attributed to the ligand field^{26,27} and these metal ions are d^{10} configuration.

Determination of Biological Activity

The prepared compounds were screened for four bacterial strains (*S. aureus*, *B. subtilis*, *E. coli*, and *P. aeruginosa*) using the disc diffusion method (Table 5). The tested compounds indicated all compounds have antimicrobial activity against all tested bacteria.²⁸

CONCLUSION

This work deals with the formation and characterization of the Schiff-base ligand and its complexes were. The reaction of (1R, 2R, 4R, 5S)-2,4-diphenyl-3-azabicyclo [3.3.1] nonan-9-one (M_1) with furan-2-carbohydrazide in the presence of EtOH and a few drops of conc. HCl resulted in the isolation of the title ligand. The formation of metal complexes was achieved from the reaction of the Schiff-base ligand with some metal ions. The predicted structures of the ligand and complexes along with the suggested geometry about the metal centre were concluded via spectroscopic and analytical techniques. These results showed the geometry of Cr(III), Mn(II) and Ni(II) metal centres are distorted octahedral. Further, the suggested geometry about the metal centre in the complex of Cu(II) is a square planar. Complexes of Zn(II) and Cu(II) indicated tetrahedral geometry about the metal centre. The biological assay of the prepared compounds against four bacteria strains showed all compounds exhibited excellent activity.

REFERENCES

- Al-Rubaye BK, Brink A, Miller GJ, Potgieter H, Al-Jeboori MJ. Crystal structure of (E)-4-benzylidene-6-phenyl-1, 2, 3, 4, 7, 8, 9, 10-octahydrophenanthridine. Acta Crystallographica Section E: Crystallographic Communications. 2017 Jul 1;73(7):1092-6.
- Al-Rubaye BK, Potgieter H, Al-Jeboori MJ. An Efficient One-Pot Approach for the Formation of Phenanthridine Derivative; Synthesis and Spectral Characterisation. Der Chemica Sinica. 2017;8(3):365-70.
- Subramaniapillai SG. Mannich reaction: A versatile and convenient approach to bioactive skeletons. Journal of Chemical Sciences. 2013 May;125(3):467-82.
- T. H. Mawat and M. J. Al-Jeboori, Journal of Molecular Structure, (2020), 1208, 127867.
- T. H. Mawat and M. J. Al-Jeboori, Journal of Global Pharma Technology, (2019), 11(09), (Suppl.), 126-138.
- B. K. Al-Rubaye, PhD Thesis, University of Baghdad, College of Education for Pure Sciences, (2017), (Ibn-Al-Haitham).

7. J. W. Gooch, Springer Science & Business Media, Vol. 1. (2010).
8. J. F. Allochio, R. G. Fiorot, M. Delarmelin, V. Lacerda, R. B. Santos and S. J. Greco, *Orbital: The Electronic Journal of Chemistry*, (2013), 5 (2): p. 96-142.
9. W. Sreevalli, G. Ramachandran, W. Madhuri and K. Sathiyarayanan, *Mini-Reviews in Organic Chemistry*, (2014), 11 (1): p. 97-11.
10. H. A. Saleh, A-S Al-Khatib and M. J. Al-Jeboori, *Biochem. Cell. Arch.*, (2021), 21 (1):p. 159-168.
11. M. J. Al-Jeboori, M. S. Al-Fahdawi and A. A. Sameh, *J. Coord. Chem.*, (2009), 62, 3853-3863.
12. B. K. Al-Rubaye, H. Potgieter and M. J. Al-Jeboori, *Journal of Physics: Conference Series*, IOP Publishing, (2021), 1879 , 022074.
13. R. M. Silverstein, G. C. Basslev and T. C. Morrill, 4thEdn., John Wiley and Sons. New York, (1981), 172.
14. S. A. Hussain and M. J. Al-Jeboori, *Journal of Global Pharma Technology*, (2019), 11(2), 548-560.
15. M. J. Al-Jeboori, F. A. Al-Jebouri and M. A. R. Al-Azzawi, *Inorg. Chim. Acta*, (2011), 379, 163-170.
16. M. Liaqat, T. Mahmud, M. Imran, M. Iqbal, M. Muddassar, T. Ahmad and L. Mitu, *Revista de Chimie*, (2017), 68 (11), 1-6.
17. M. J. Al-Jeboori, H. H. Al-Tawel and R. M. Ahmed, *Inorg. Chim. Acta*, (2010), 363, p. 1301-1305.
18. A. J. Abdul-Gganiy, M. J. Al-Jeboori and J. A. Al-karawi *Journal of Coordination Chemistry*, (2009), 62, 2736.
19. T. H. Mawat, and M. J. Al-Jeboori, *Biochem. Cell. Arch.*, (2019), 19(2), 4573-4580.
20. H. A. Salman, A. A. Abdul Rahman and M. J. Al-Jeboori, *Biochem. Cell. Arch.*, (2021). 21(1), 159-168.
21. K. Nisah, M. RamLi, R. Idroes, A. Safitri, *IOP Conference Series: Materials Science and Engineering*. (2021), Vol. 1087. No. 1. IOP Publishing.
22. M. J. Al-Jeboori, A. J. Abdul-Ghani and A. J. Al-Karawi, *Transition Met. Chem.*, (2008), 33, p. 925-930.
23. T. H. Mawat, MSc Thesis, University of Baghdad, College of Education - Ibn-Al-Haitham, (2016).
24. A. Lever, *Inorganic Electronic Spectroscopy*, 2, p. 376-611, (1984).
25. E. I. Yousif, PhD Thesis, University of Baghdad, College of Education for Pure Sciences (Ibn-Al-Haitham), (2016).
26. A. H. Abdulhadi and M. J. Al-Jeboori, *Biochem. Cell. Arch.*, (2020), 20, 4207-4216.
27. R. M. Ahmed, B. K. Al-Rubaye, N. J. Hussien, E. I. Yousif, H. A. Hassan and M. J. Al-Jeboori, *International Journal of Pharmaceutical Research*, p. (2021), 2251-2260.
28. R. Ramesh and S. Maheswaran, *J. Inorg. Biochem.*, (2003), 96, p. 457-462.